FTIR Study of the Photoisomerization Processes in the 13-*cis* and All-*trans* Forms of *Anabaena* Sensory Rhodopsin at 77 K†

Akira Kawanabe,‡ Yuji Furutani,‡,§ Kwang-Hwan Jung,|| and Hideki Kandori*,‡,§

Department of Materials Science and Engineering, Nagoya Institute of Technology, Showa-ku, Nagoya 466-8555, Japan, Core Research for Evolutional Science and Technology (CREST), Japan Science and Technology Corporation, Kyoto 606-8502, Japan, and Department of Life Science and Interdisciplinary Program of Integrated Biotechnology, Sogang University, Shinsu-Dong 1, Mapo-Gu, Seoul 121-742, Korea

Received November 14, 2005; Revised Manuscript Received February 10, 2006

ABSTRACT: Archaeal-type rhodopsins can accommodate either all-*trans*- or 13-*cis*,15-*syn*-retinal in their chromophore binding site in the dark, but only the former isomer is functionally important. In contrast, *Anabaena* sensory rhodopsin (ASR), an archaeal-type rhodopsin found in eubacteria, exhibits a photochromic interconversion of both forms, suggesting that ASR functions as a photosensor which interacts with its 14 kDa soluble transducer differently in the all-*trans* and 13-*cis*,15-*syn* forms. In this study, we applied low-temperature Fourier transform infrared (FTIR) spectroscopy to the 13-*cis*,15-*syn* form of ASR (13C-ASR) at 77 K and compared the local structure around the chromophore and its structural changes upon retinal photoisomerization with those of the all-*trans* form (AT-ASR) [Furutani, Y., Kawanabe, A., Jung, K. H., and Kandori, H. (2005) *Biochemistry 44*, 12287−12296]. By use of [ζ-^{15}N]-lysine-labeled ASR, we identified the N−D stretching vibrations of the Schiff base (in D_2O) at 2165 cm^{-1} for 13C-ASR and at 2163 and 2125 cm^{-1} for AT-ASR. The frequencies indicate strong hydrogen bonds of the Schiff base with a water molecule for both 13C-ASR and AT-ASR. In contrast, the N−D stretching vibration appears at 2351 cm^{-1} and at 2483 cm^{-1} for the K states of 13C-ASR (13C-ASR_K) and AT-ASR (AT-ASR_K), respectively, indicating that the Schiff base still forms a hydrogen bond in 13C-ASR_K. Rotational motion of the Schiff base upon retinal isomerization is probably smaller for 13C-ASR than for AT-ASR, the latter altering hydrogen bonding of the Schiff base similar to bacteriorhodopsin (BR), a light-driven proton pump. Appearance of several hydrogen-out-of-plane vibrations and amide I vibrations in 13C-ASR_K, but not in AT-ASR_K, suggests that structural changes are distributed widely along the polyene chain for 13C-ASR. On the other hand, retinal photoisomerization in AT-ASR breaks the hydrogen bond of the Schiff base, and localized structural changes in the Schiff base region are induced.

Four archaeal-type rhodopsins [bacteriorhodopsin (BR),[1] halorhodopsin (HR), sensory rhodopsin (SR) (also called sensory rhodopsin I), and phoborhodopsin (pR) (also called sensory rhodopsin II)] were discovered in the cytoplasmic membrane of *Halobacterium salinarum* (*1*−*4*). The former two rhodopsins (BR and HR) function as light-driven proton and chloride pumps, respectively, while the latter two rhodopsins (SR and pR) act as photosensors responsible for attractant or repellent phototaxis, respectively. They have been extensively studied as model systems converting light energy into electrochemical potential or relaying environmental signal into the cytoplasm. Although such rhodopsins were believed to exist only in Archaea, genome sequencing projects and environmental genomics have recently revealed that archaeal-like rhodopsins also exist in Eukarya and Eubacteria. In eucaryotes, archaeal rhodopsins were found in fungi (*5*), green algae (*6*, *7*), dinoflagellates (*8*), and cryptomonads (*9*). Eubacterial rhodopsins were found in γ- and α-proteobacteria (*10*−*12*) as well as in *Anabaena* (*Nostoc*) sp. PCC7120, a freshwater cyanobacterium (*13*), where it was named *Anabaena* sensory rhodopsin (ASR).

The gene encoding ASR, which is a membrane protein of 261 residues (26 kDa), and a small gene encoding a soluble protein of 125 residues (14 kDa) are under the same promoter in a single operon (*13*). The opsin gene was expressed heterologously in *Escherichia coli* and upon binding of all-*trans*-retinal formed a pink pigment (λ_{max} 549 nm in the dark-adapted form) with a photochemical reaction cycle of 110 ms half-life (pH 6.8, 18 °C) (*13*). The previous study reported that coexpression with the 14 kDa protein accelerated the photocycle, indicating physical interaction with ASR (*13*). This fact suggested that ASR has a photosensory function

† This work was supported in part by grants from the Japanese Ministry of Education, Culture, Sports, Science, and Technology to H.K. (15076202) and by Research Fellowships from the Japan Society for the Promotion of Science for Young Scientists to Y.F.

* To whom correspondence should be addressed. Phone/Fax: 81-52-735-5207. E-mail: kandori@nitech.ac.jp.

‡ Nagoya Institute of Technology.

§ CREST.

|| Sogang University.

[1] Abbreviations: BR, bacteriorhodopsin; HR, halorhodopsin; SR, sensory rhodopsin; pR, phoborhodopsin; ASR, *Anabaena* sensory rhodopsin; λ_{max}, maximum absorption wavelength; AT-ASR, *Anabaena* sensory rhodopsin possessing all-*trans*-retinal as the chromophore; 13C-ASR, *Anabaena* sensory rhodopsin possessing 13-*cis*-retinal as the chromophore; HPLC, high-performance liquid chromatography; DM, *n*-dodecyl β-D-maltoside; PC, L-α-phosphatidylcholine; *p*pR, *pharaonis* phoborhodopsin (*Natronomonas pharaonis* sensory rhodopsin II); 13C-ASR_K, the K intermediate of 13C-ASR; AT-ASR_K, the K intermediate of AT-ASR; HOOP, hydrogen-out-of-plane vibration.

10.1021/bi052324b CCC: $33.50
Published on Web 03/15/2006

rather than a bioenergetic one. According to the recent X-ray crystal structure, ASR accommodates both all-*trans*- and 13-*cis*,15-*syn*-retinal in the ground state, which can be interconverted by illumination with blue (480 nm) or orange (590 nm) light (*14*). Such photochromic behavior is never observed in BR, HR, SR, and pR. These results might suggest that ASR is a photochromic color sensor.

To understand the details of light-induced structural changes of ASR, we have recently applied low-temperature FTIR spectroscopy to the all-*trans* form of ASR (AT-ASR) and compared the difference spectra at 77 K with those of BR (*15*). The K intermediate minus AT-ASR difference spectra showed that the retinal isomerizes from all-*trans* to distorted 13-*cis* form similar to BR. On the other hand, a remarkable difference between AT-ASR and BR was revealed in water bands. Although ASR possesses a water molecule between the Schiff base and its counterion Asp75 similar to BR, the O−D stretching bands of water molecules were observed only in the >2500 cm^{-1} region for AT-ASR (*15*). We interpreted that the weak hydrogen bond of the bridged water in ASR originates from its unique geometry. Since ASR does not pump protons and the direction of the proton movement is toward cytoplasmic side from the characteristics of the photoelectric signal (*16*), the results support the working hypothesis that the existence of strongly hydrogen-bonded water molecules is essential for proton pumping activity in archaeal rhodopsins (*17*).

In the present paper, we extended the low-temperature spectroscopic study at 77 K to the 13-*cis*,15-*syn* form of ASR (13C-ASR). HPLC analysis revealed that light-adapted ASR with light >560 nm at 4 °C possesses 78% 13C-ASR, while dark-adapted ASR has AT-ASR predominantly (97%). Then, we established the illumination conditions to measure the difference spectra between 13C-ASR and its K state without subtracting the difference between AT-ASR and its K state. Spectral comparison between 13C-ASR and AT-ASR provided useful information on structure and structural changes upon retinal photoisomerization in ASR. In particular, previous X-ray crystallographic study of ASR reported the same protein structure for 13C-ASR and AT-ASR (*14*), whereas the present FTIR study revealed that protein structural changes upon retinal photoisomerization were significantly different between 13C-ASR and AT-ASR. The differences were seen for HOOP modes of the retinal chromophore, amide I, cysteine S−H stretch, the Schiff base N−D stretch, and water O−D stretch modes. These must trigger different global protein structural changes in each photoreaction cycle leading to the observed photochromic behavior.

MATERIALS AND METHODS

Sample Preparation. Samples for the present spectroscopic analysis were prepared as described previously (*13*, *18*). Briefly, *E. coli* strain BL21 (Stratagene) was transformed by introducing pMS107-derivative plasmid (*13*), which encodes the *Anabaena* opsin, and was grown in 2× YT medium in the presence of ampicillin (50 μg/mL) at 38 °C. Three hours after IPTG induction with addition of 10 μM all-*trans*-retinal, pink-colored cells were harvested, sonicated, solubilized by 1% DM, and purified by a Ni^{2+}-NTA column. The purified ASR was then reconstituted into PC liposomes by removing the detergent with Bio-Beads, where the molar ratio of the added PC to ASR was 50:1. The liposomes were washed three times with a buffer [2 mM sodium phosphate (pH 7.0)]. A 60 μL aliquot was deposited on a BaF_2 window of 18 mm diameter and dried in a glass vessel that was evacuated by an aspirator. [ζ-^{15}N]Lysine-labeled ASR was prepared as was done for [ζ-^{15}N]lysine-labeled *pharaonis* phoborhodopsin (*p*pR) (*19*).

HPLC Analysis. HPLC analysis was performed as described previously (*20*). A high-performance liquid chromatograph was equipped with a silica column (6.0 × 150 mm; YMC-Pack SIL). The solvent was composed of 12% (v/v) ethyl acetate and 0.12% (v/v) ethanol in hexane, and the flow rate was 1.0 mL/min. Extraction of retinal oxime from the sample was carried out by hexane after denaturation by methanol and 500 mM hydroxylamine at 4 °C (*21*). The molar composition of retinal isomers was calculated from the areas of the peaks in the HPLC patterns. Assignment of the peaks was performed by comparing them with the HPLC pattern from retinal oximes of authentic all-*trans*- and 13-*cis*-retinals. Three independent measurements were averaged.

FTIR Spectroscopy. FTIR spectroscopy was performed as described previously (*18*). The ASR film sample was hydrated with 1 μL of H_2O, D_2O, or $D_2{}^{18}O$ before the measurements. Then, the sample was placed in a cryostat (DN-1704; Oxford) mounted in the FTIR spectrometer (FTS-40; Bio-Rad). The cryostat was equipped with a temperature controller (ITC-4; Oxford), and the temperature was regulated with 0.1 K precision. To accumulate 13C-ASR, we established the following conditions for the light adaptation. Hydrated films were illuminated with >560 nm light (O-58 cutoff filter; Toshiba) from a 1 kW halogen−tungsten lamp for 1 min at 4 °C. HPLC analysis showed that the light-adapted ASR possesses 78% 13-*cis* and 22% all-*trans* forms. The sample was cooled for 3 min after the light adaptation to allow for the complete decay of photoproducts.

Light-adapted ASR contains both all-*trans* and 13-*cis* forms, thus, its photoreactions strongly depend on the illumination wavelength. In this study, we established the following illumination conditions to obtain the K intermediate of 13C-ASR (13C-ASR_K) minus 13C-ASR spectra at 77 K. Illumination with 501 nm light for 1 min first converted 13C-ASR to 13C-ASR_K together with the conversion of AT-ASR to the K intermediate of AT-ASR (AT-ASR_K). Nevertheless, subsequent illumination at >560 nm (O-58 cutoff filter; Toshiba) reverted only 13C-ASR_K to 13C-ASR, whereas no photoreversion was found for AT-ASR_K. In the previous study for AT-ASR, we illuminated AT-ASR_K at >590 nm for the photoreversion to AT-ASR (*15*). The present result indicates that illumination at >560 nm does not change the photoequilibrium between AT-ASR and AT-ASR_K. Subsequent illuminations by 501 nm light and >560 nm light do not induce the spectral features of AT-ASR_K minus AT-ASR. Each difference spectrum was calculated from the two spectra constructed from 128 interferograms taken before and after the illumination. Twenty-four (H_2O and D_2O) or forty-eight ($D_2{}^{18}O$) difference spectra were obtained and averaged to produce the 13C-ASR_K minus 13C-ASR spectrum. ASR molecules are randomly oriented in the liposome film as confirmed by linear dichroism experiments, so we did not apply dichroic measurements using an IR polarizer.

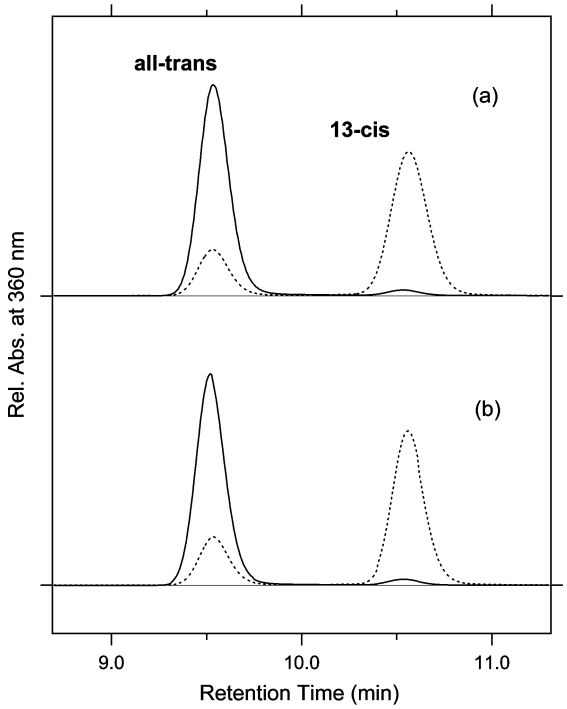

FIGURE 1: HPLC of chromophores extracted from ASR in DM micelles (a) and in PC liposomes (b). The detection beam was set at 360 nm. After the extraction, retinal oxime exists in 15-*syn* and 15-*anti* forms. In the range of retention times shown, only the 15-*syn* form appears. We used the area of both 15-*syn* and 15-*anti* forms for calculation of isomeric ratios. Dark-adapted ASR (solid lines) is in the all-*trans* form predominantly [AT-ASR; 95.5 ± 0.8% in (a) and 97.1 ± 0.1% in (b)], while light-adapted ASR (dotted lines) possesses more of the 13-*cis* form [13C-ASR; 78.1 ± 1.2% in (a) and 77.9 ± 1.7% in (b)].

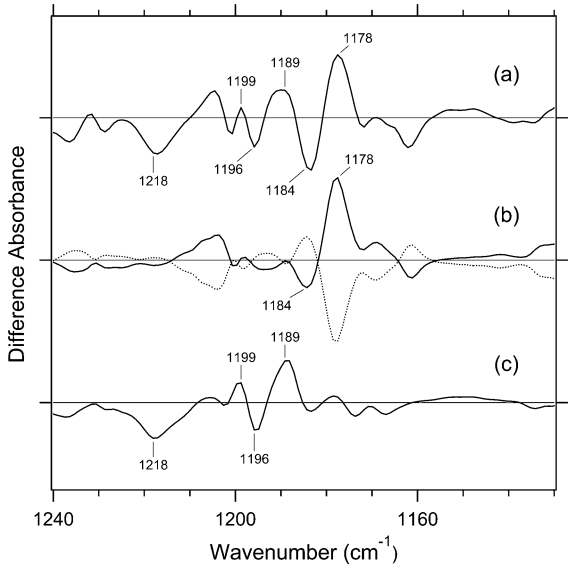

FIGURE 2: Difference FTIR spectra in the 1240−1130 cm^{-1} region measured at 77 K (in H_2O), where the spectra before illumination were subtracted from those after illumination. Light-adapted ASR that contains 13C-ASR (78%) and AT-ASR (22%) was first illuminated with 501 nm light for 1 min (a). Then, illumination at >560 nm for 1 min converted a part of the photoproducts in (a) to the original state [dotted line in (b)]. Subsequent illumination with 501 nm light yields the difference spectrum [solid line in (b)], which is a mirror image of the dotted spectrum. Repeated illuminations at >560 nm and at 501 nm yield the identical spectra. (c) The AT-ASR_K minus AT-ASR spectra are reproduced from Furutani et al. (*15*). One division of the *y*-axis corresponds to 0.005 absorbance unit.

RESULTS

Dark-adapted ASR is predominantly in the all-*trans* form, while the light adaptation process increases concentration of the 13-*cis* form (*14*, *22*). This is in contrast to the case of BR, where light adaptation leads to a complete conversion into the all-*trans* form (*23*). In this study, we attempted to establish the illumination conditions to accumulate the 13-*cis* form for DM-solubilized and PC-liposome-based ASR samples, using HPLC column chromatography. Panels a and b of Figure 1 show that the dark-adapted ASR (solid lines) possesses 95.5% and 97.1% all-*trans* form for the DM-solubilized and PC-liposome-based samples, respectively. On the other hand, illumination of ASR with >560 nm light for 1 min at 4 °C results in accumulation of 13C-ASR. HPLC analysis showed that the light-adapted ASR possesses 78.1% and 77.9% of the 13-*cis* form for the DM-solubilized and PC-liposome-based samples, respectively. Thus, the isomeric composition was not influenced by the reconstitution. Dark adaptation was a slow process, with half-time >1 h at 4 °C (data not shown).

A hydrated film of ASR in PC liposomes was light-adapted as described above and then cooled to 77 K, followed by illumination at 501 nm. Figure 2a shows the light minus dark difference FTIR spectra of the light-adapted ASR. Vibrational bands at 1218 (−), 1199 (+), 1196 (−), and 1189 (+) cm^{-1} also appear in the AT-ASR_K minus AT-ASR (Figure 2c) (*15*), indicating that the conversion of AT-ASR to AT-ASR_K is involved in the spectrum of Figure 2a. On the other hand, Figure 2a possesses additional strong peaks at 1184 (−) and 1178 (+) cm^{-1}, suggesting the involvement of the photoreaction of 13C-ASR. In the previous study for AT-ASR, we illuminated AT-ASR_K at >590 nm for the photoreversion to AT-ASR (*15*). In the present study, subsequent illuminations at >560 and 501 nm yielded the spectra shown in Figure 2b (dotted and solid lines, respectively). Lack of the bands at 1218, 1199, 1196, and 1189 cm^{-1} strongly suggests that the spectra do not contain the photoreaction of AT-ASR. In other words, the solid line in Figure 2b corresponds to the 13C-ASR_K minus 13C-ASR spectrum. In fact, the spectrum of Figure 2a is well constructed from the solid lines in Figure 2b,c (data not shown). In this way, we obtained the 13C-ASR_K minus 13C-ASR difference FTIR spectra without any subtraction of spectral contribution from AT-ASR. It is likely that the photoequilibrium between AT-ASR and AT-ASR_K is not changed between illuminations at 501 nm and at >560 nm, so that further illumination with 501 nm and >560 nm in Figure 2b yielded the difference spectra between 13C-ASR and 13C-ASR_K.

Comparison of the Difference Infrared Spectra of the Photoreactions of 13C-ASR and AT-ASR at 77 K in the 1770−870 cm^{-1} Region. Figure 3 shows the 13C-ASR_K minus 13C-ASR (a) and the AT-ASR_K minus AT-ASR spectra (b), which were measured at 77 K upon hydration with H_2O (solid lines) and D_2O (dotted lines). In Figure 3a, the negative band at 1539 cm^{-1} corresponds to the ethylenic stretching vibration of the 13-*cis* chromophore in ASR, which exhibits the absorption maximum at 537 nm (*14*). The frequency is in good agreement with the well-known linear correlation between the ethylenic stretching frequencies and absorption maxima for various retinal proteins (*24*). Il-

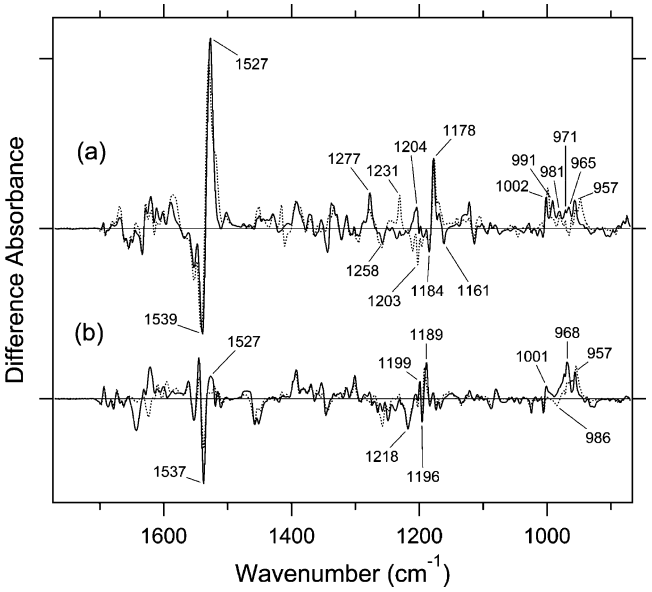

FIGURE 3: The 13C-ASR$_K$ minus 13C-ASR (a) and the AT-ASR$_K$ minus AT-ASR (b) spectra (pH 7) in the 1770−870 cm^{-1} region measured at 77 K upon hydration with H_2O (solid line) and D_2O (dotted line), respectively. The spectra in panel b are reproduced from Furutani et al. (*15*). One division of the *y*-axis corresponds to 0.007 absorbance unit.

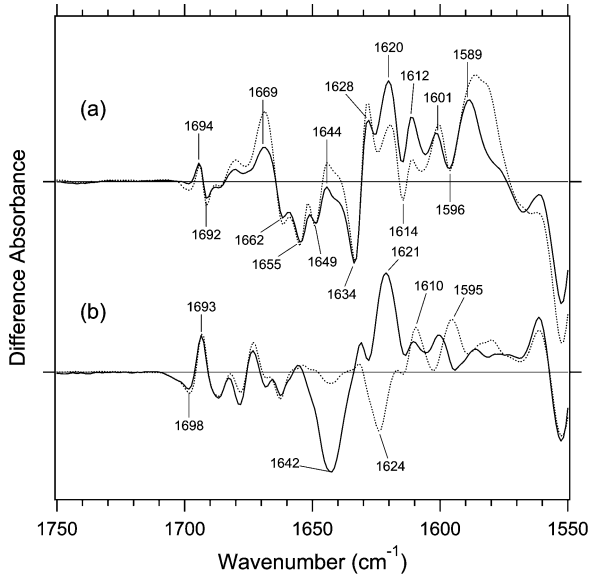

FIGURE 4: The 13C-ASR$_K$ minus 13C-ASR (a) and the AT-ASR$_K$ minus AT-ASR (b) spectra (pH 7) in the 1750−1550 cm^{-1} region, mostly representing vibrations of the protein moiety. The sample was hydrated with H_2O (solid lines) or D_2O (dotted lines). One division of the *y*-axis corresponds to 0.0025 absorbance unit.

lumination results in the spectral downshift to 1527 cm^{-1}, indicating formation of the red-shifted K intermediate (13C-ASR$_K$).

C−C stretching vibrations of the retinal in the 1300−1150 cm^{-1} region are sensitive to the local structure of the chromophore. In the 13C-ASR$_K$ minus 13C-ASR spectrum in H_2O, peaks are observed at 1277 (+), 1258 (−), 1204 (+), 1184 (−), 1178 (+), and 1161 (−) cm^{-1} (Figure 3a, solid line). In the case of the 13-*cis* form of BR, appearance of a peak pair at 1185 (−) and 1177 (+) cm^{-1} was regarded as a marker of the formation of the all-*trans* photoproduct (*25*). Similar bands at 1184 (−) and 1178 (+) cm^{-1} for 13C-ASR strongly suggest that 13C-ASR$_K$ possesses the all-*trans* chromophore produced by photoisomerization of the C13═C14 bond. As in the case of BR, the 1184 (−)/1178 (+) cm^{-1} bands are insensitive to the H−D exchange (Figure 3a, dotted line), being thus assignable to C10−C11 stretching vibration (*25*). Strong positive peaks at 1277 and 1204 cm^{-1} in H_2O and at 1231 cm^{-1} in D_2O were also observed for the 13-*cis* form of BR, where positive peaks at 1205 cm^{-1} in H_2O and at 1234 cm^{-1} in D_2O were assigned to be C14−C15 stretching vibrations (*25*). Therefore, corresponding peaks at 1204 cm^{-1} in H_2O and at 1231 cm^{-1} in D_2O are assignable to the C14−C15 stretching vibration of 13C-ASR$_K$. Spectral coincidence between BR and ASR implies similar chromophore structures of their 13-*cis* forms and respective K states.

Hydrogen-out-of-plane (HOOP), N−D in-plane bending, and methyl rocking vibrations are observed in the 1110−890 cm^{-1} region, and the presence of strong HOOP modes represents distortions of the retinal molecule (*26*). The AT-ASR$_K$ minus AT-ASR spectra exhibit two strong peaks at 968 and 957 cm^{-1} (Figure 3b). In contrast, many positive bands were observed in the 13C-ASR$_K$ minus 13C-ASR spectra, whose frequencies are at 1002, 991, 981, 971, 965, and 957 cm^{-1} (Figure 3a). This observation suggests that the chromophore of 13C-ASR$_K$ is more distorted along the polyene chain than that of AT-ASR$_K$.

Figure 4 shows the 13C-ASR$_K$ minus 13C-ASR (a) and the AT-ASR$_K$ minus AT-ASR spectra (b) in the 1750−1550 cm^{-1} region. Amide I vibrations appear in this frequency region together with the C═N stretching vibration of the protonated retinal Schiff base. In general, the former is insensitive to the H−D exchange, whereas the latter exhibits downshift in D_2O. In the case of AT-ASR, a prominent peak pair at 1642 (−) and 1621 (+) cm^{-1} is assignable to the C═N stretchings of AT-ASR and AT-ASR$_K$, respectively, because of the spectral shifts to 1624 (−) and 1610 (+) cm^{-1} in D_2O (Figure 4b). In fact, we observed the downshift of the bands at 1642 (−) and 1621 (+) cm^{-1} by 10 cm^{-1} for [ζ-^{15}N]lysine-labeled ASR, indicating that they originate from the C═N stretching vibrations (data not shown). It should be noted that the spectral changes of amide I vibrations at 1660−1630 cm^{-1} are small in AT-ASR$_K$ minus AT-ASR, which is clearly seen in D_2O (Figure 4b, dotted line), suggesting that no structural changes of the peptide backbone occur in AT-ASR upon retinal isomerization.

The spectral features are quite different for 13C-ASR. Figure 4a shows the presence of the H−D exchange-independent bands in the 1660−1630 cm^{-1} region, located at 1669 (+), 1662 (−), 1655 (−), 1649 (−), 1644 (+), 1634 (−), and 1628 (+) cm^{-1}. This suggests perturbation of the peptide backbone upon retinal photoisomerization of 13C-ASR. In particular, the peaks at 1662, 1655, and 1649 cm^{-1} are ascribable to the amide I vibrations of the α-helix. Helical perturbation may be correlated with many peaks of the HOOP vibrations in 13C-ASR$_K$.

Unlike in AT-ASR (Figure 4b), the 13C-ASR$_K$ minus 13C-ASR spectra (Figure 4a) do not show H−D exchange-dependent bands clearly. This indicates that the C═N stretching vibrations are not clearly observed in the spectra. Reproducible differences between H_2O and D_2O samples in Figure 4a suggest that the C═N stretching vibrations are present in this frequency region. In fact, bands at 1640−

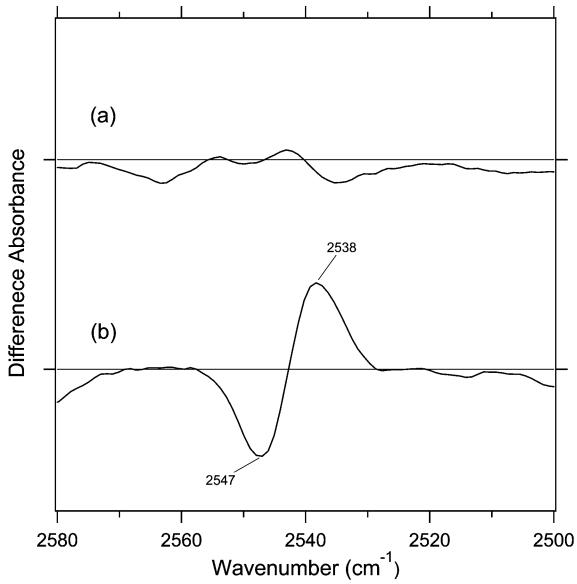

FIGURE 5: The 13C-ASR_K minus 13C-ASR (a) and the AT-ASR_K minus AT-ASR (b) spectra (pH 7) in the 2580−2500 cm^{-1} region, which correspond to S−H stretching vibrations of cysteine residues. The sample was hydrated with H_2O. One division of the *y*-axis corresponds to 0.0003 absorbance unit.

1620 cm^{-1} were sensitive to [ζ-^{15}N]lysine labeling (not shown). However, the absence of clear peaks of the C═N stretch requests spectral analysis using double difference spectra. The C═N stretching vibrations have been regarded as an important marker, because the difference in frequency between H_2O and D_2O samples probes hydrogen-bonding strength of the Schiff base (*27*, *28*). In the present study, however, we discuss the hydrogen-bonding strength of the Schiff base by use of the N−D stretching in D_2O (see below), which is the more direct probe (*29*).

In the carboxylic C═O stretching frequency region (>1700 cm^{-1}), there are no bands for 13C- and AT-ASR_K (Figures 3 and 4). This implies that Asp and Glu residues are located far from the retinal even if they are protonated. In the BR_K minus BR difference spectra, the bands at 1742 (−) and 1733 (+) cm^{-1} were assigned to the C═O stretching vibrations of the protonated Asp115 (*30*). ASR has a glutamine residue (Gln109) at the corresponding position, whose vibrational bands are probably observed at 1698 (−) and 1693 (+) cm^{-1} for AT-ASR (Figure 4b). Similar bands were also observed at 1704 (−) and 1700 (+) cm^{-1} in the difference spectra of *p*pR, which has an asparagine residue at the corresponding position (*31*). Therefore, it can be suggested that the structural changes occurring around Asp115 in BR are common for ASR, BR, and *p*pR. Figure 4a shows the bands at 1694 (+) and 1692 (−) cm^{-1} for 13C-ASR, which can be assigned to the C═O stretch of Gln109. It is likely that the C═O stretching vibrations of Asp115 in BR are dependent on the isomeric form as well.

S−H Stretching Vibrations of Cysteine Residues. Figure 5 shows the 13C-ASR_K minus 13C-ASR (upper panel) and AT-ASR_K minus AT-ASR (lower panel) spectra in the 2580−2500 cm^{-1} region, which corresponds to S−H stretching vibration of cysteine. As we already reported, there is a negative band at 2547 cm^{-1} and a positive band at 2538 cm^{-1} for AT-ASR (Figure 5b). In contrast, no spectral changes were observed for 13C-ASR, indicating that the 13-*cis* to all-*trans* isomerization in ASR does not alter the local structure of cysteines (Figure 5a). There are three cysteine residues in ASR, Cys134 and Cys137 in helix E and Cys203 in helix G. None of them is conserved in archaeal-type rhodopsins. The cysteines were replaced by alanines, producing proteins with absorption maxima at 546 nm for the wild type, 548 nm for C134A, 546 nm for C137A, and 553 nm for C203A (measured for DM-solubilzed ASR at pH 7.0; unpublished data). The X-ray crystal structure of ASR also revealed that only the S−H group of Cys203 points to the inside of the protein in the Schiff base region consistent with the fact that the mutation at this position influences the absorption maximum. We suggested previously that the observed vibrational bands may be assignable to the S−H stretching of Cys203 (*15*).

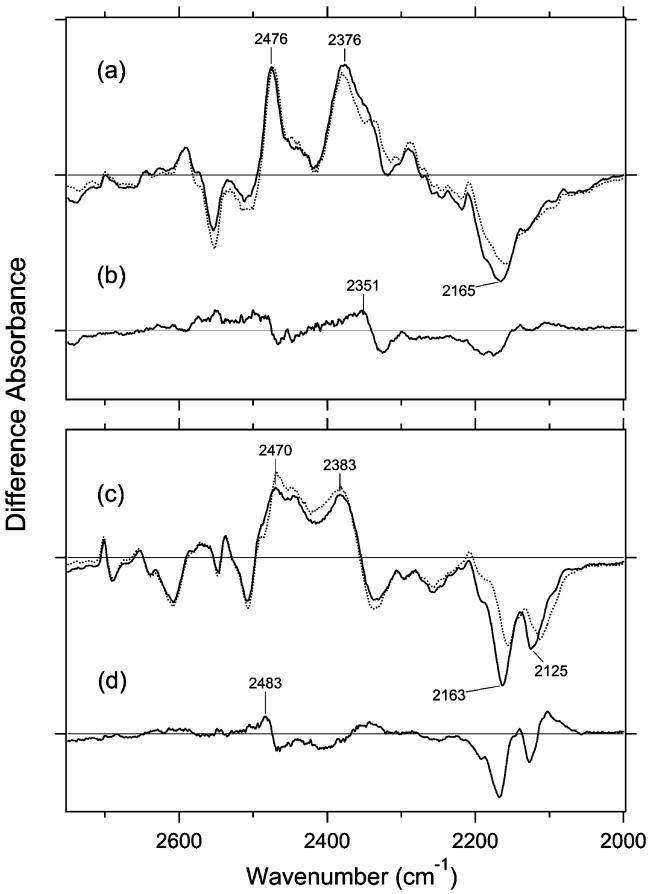

FIGURE 6: The 13C-ASR_K minus 13C-ASR (a) and the AT-ASR_K minus AT-ASR (c) spectra (pH 7) in the 2750−2000 cm^{-1} region for [ζ-^{15}N]lysine-labeled (dotted line) and unlabeled (solid line) ASR. Double difference spectra in (a) and (c) (solid line minus dotted line) are shown in (b) and (d), respectively. The samples were hydrated with D_2O, and spectra were measured at 77 K. One division of the *y*-axis corresponds to 0.0007 absorbance unit.

Assignment of the N−D Stretching Vibrations in 13C-ASR and AT-ASR. X−D stretching vibrations of protein and water molecules appear in the 2750−2000 cm^{-1} region for the films hydrated with D_2O (Figure 6). The solid line of Figure 6c shows the AT-ASR_K minus AT-ASR spectrum reported earlier (*15*). On the other hand, the 13C-ASR_K minus 13C-ASR spectrum (solid line of Figure 6a) is obtained for the first time. Since the N−D stretching vibrations of the Schiff base should be present in this frequency region, we then attempted to assign them by use of the [ζ-^{15}N]lysine-labeled ASR sample.

Figure 6a compares the 13C-ASR$_K$ minus 13C-ASR spectra between [ζ-^{15}N]lysine-labeled (dotted line) and unlabeled (solid line) ASR. Clear isotope-induced spectral downshift was observed for intense positive and negative bands at 2376 and 2165 cm^{-1}, respectively. Other bands are identical between [ζ-^{15}N]lysine-labeled and unlabeled 13C-ASR. Thus, we are able to conclude that the N−D stretching vibrations of the Schiff base are present in this frequency region. It should however be noted that the strong positive peak at 2376 cm^{-1} probably contains other vibrations because the isotope effect was observed in the broad range of 2370−2320 cm^{-1} (Figure 6a). In fact, the AT-ASR$_K$ minus AT-ASR spectra contain such peak at 2383 cm^{-1} as well (Figure 6c), which may originate from amide A vibrations. By use of double difference spectra from the data shown in Figure 6a, we determined that the N−D stretching vibration of the Schiff base in 13C-ASR$_K$ is located at 2351 cm^{-1} (Figure 6b).

Figure 6c compares the AT-ASR$_K$ minus AT-ASR spectra between [ζ-^{15}N]lysine-labeled (dotted line) and unlabeled (solid line) ASR. Clear isotope-induced spectral downshift was observed for the two negative bands at 2163 and 2125 cm^{-1}, indicating that the bands originate from N−D stretching vibrations of the Schiff base in AT-ASR. Additionally, the positive spectral feature at 2470 cm^{-1} exhibits isotope shift from [ζ-^{15}N]lysine labeling as well. By use of double difference spectra from the data shown in Figure 6c, we determined that the N−D stretching vibration of the Schiff base in AT-ASR$_K$ is located at 2483 cm^{-1} (Figure 6d). The positive peak at 2470 cm^{-1} probably contains other vibrations such as the O−D stretching vibrations of Thr79. In BR, the O−D frequencies of Thr89, the homologue of Thr79 in ASR, are 2507 and 2466 cm^{-1} for BR and BR$_K$, respectively (*32*). A similar positive band was also observed at 2476 cm^{-1} for 13C-ASR (Figure 5a).

Thus, by use of [ζ-^{15}N]lysine-labeled ASR, we identified the N−D stretching vibrations of the Schiff base at 2163 and 2125 cm^{-1} for AT-ASR and at 2165 cm^{-1} for 13C-ASR. This indicates that the hydrogen-bonding strength is very similar for the two isomeric forms, being slightly stronger in AT-ASR. The X-ray crystallographic structure reported the presence of a water molecule in contact with the Schiff base, making it a good candidate for the hydrogen-bonding acceptor (*14*). Similarity of the hydrogen bonding in AT-ASR and 13C-ASR is consistent with the X-ray structure.

We also identified the N−D stretching vibration of the Schiff base at 2483 cm^{-1} for AT-ASR$_K$ and at 2351 cm^{-1} for 13C-ASR$_K$. Upshifted N−D frequencies indicate that retinal isomerization weakens the hydrogen bond of the Schiff base for both AT-ASR and 13C-ASR. Nevertheless, unlike in the unphotolyzed states, the difference in frequencies for the K states implies the different isomerization outcomes for AT-ASR and 13C-ASR. In case of AT-ASR, the upshift of the frequency is >300 cm^{-1}, indicating that the hydrogen bond is significantly weakened (or broken) in AT-ASR$_K$, presumably because of the rotational motion of the Schiff base. In contrast, the upshift of the frequency is about 200 cm^{-1} for 13C-ASR. This fact suggests that the rotational motion of the Schiff base that accompanies retinal isomerization is smaller in 13C-ASR than in AT-ASR.

O−D Stretching Vibrations of Water in 13C-ASR and AT-ASR. A spectral comparison between the samples hydrated with D$_2$O and D$_2{}^{18}$O identifies O−D stretching vibrations of water molecules which change their frequencies upon retinal photoisomerization. We previously reported the absence of the water O−D stretch at <2500 cm^{-1} for AT-ASR (*15*). This observation was entirely different from the case of BR, being consistent with the correlation between strongly hydrogen-bonded water molecules and proton-pumping activity (*17*).

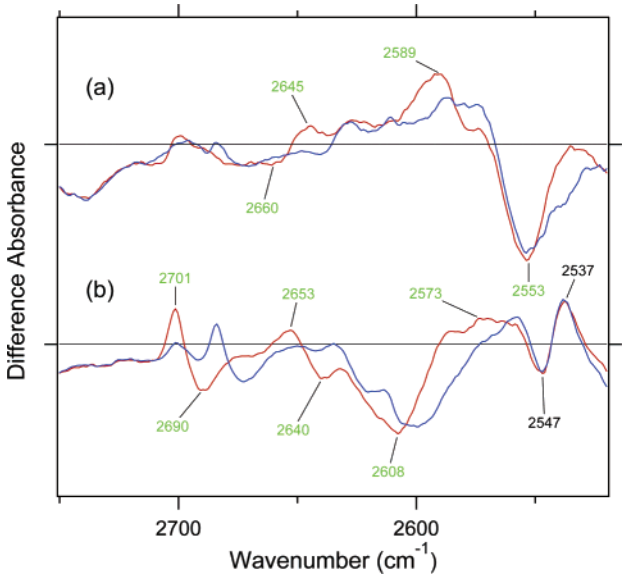

FIGURE 7: The 13C-ASR$_K$ minus 13C-ASR (a) and the AT-ASR$_K$ minus AT-ASR (b) spectra (pH 7) in the 2750−2520 cm^{-1} region measured at 77 K. The sample was hydrated with D$_2$O (red line) or D$_2{}^{18}$O (blue line). Frequencies labeled in green correspond to those identified as water stretching vibrations. One division of the *y*-axis corresponds to 0.0004 absorbance unit.

In this study, we also looked for the water bands in the 13C-ASR$_K$ minus 13C-ASR spectrum, but no water bands were found at <2500 cm^{-1} similar to AT-ASR (data not shown). This fact indicates that the bridged water molecule between the protonated Schiff base and Asp75 forms a weak hydrogen bond for both the all-*trans* and 13-*cis* form. Figure 7 shows difference FTIR spectra in the 2750−2520 cm^{-1} region, where weakly hydrogen-bonded water molecules are observed. Green-tagged bands in Figure 7 are assignable to the O−D stretching vibrations of water because of the isotope shift. Figure 7b shows that three negative peaks at 2690, 2640, and 2608 cm^{-1} were assignable to the O−D stretching vibrations of water in AT-ASR, while the bands at 2701, 2653, and 2573 cm^{-1} were assigned as water stretching vibrations of AT-ASR$_K$. The bands at 2547 (−)/ 2537 (+) cm^{-1} are attributed to the H−D unexchangeable S−H stretching vibration of a cysteine residue as shown in Figure 5b. Figure 7a shows that the bands at 2660 (−) and 2645 (+) cm^{-1} exhibit isotope shift of water. In addition, clear isotope shift was seen for the positive band at 2589 cm^{-1}. The negative band at 2553 cm^{-1} also contains water O−D stretch, though the small downshift suggests the presence of vibrations other than that of water. Therefore, two positive and two negative peaks can be assigned as O−D stretches of water in 13C-ASR.

DISCUSSION

In this study, we compared the 13C-ASR$_K$ minus 13C-ASR and AT-ASR$_K$ minus AT-ASR spectra obtained by

means of low-temperature FTIR spectroscopy. The present HPLC analysis revealed that the dark-adapted ASR is predominantly in the AT-ASR form (97%). Then, the optimal conditions of light adaptation to accumulate 13C-ASR were established, resulting in accumulation of 78% of the 13-*cis* form. This unique property of ASR raises several questions on how ASR relays the signal to its 14kDa transducer and the nature of the signaling state of ASR. If there is a structural difference between 13C-ASR and AT-ASR in the ground state, it might result in different binding affinity of the 14 kDa transducer for 13C-ASR and AT-ASR. But we cannot exclude a general mechanism in which the M state would be the signaling state as in other sensory rhodopsins. Although the light-adapted ASR contains AT-ASR, the appropriate illumination regime allowed us to obtain the 13C-ASR_K minus 13C-ASR spectra without any subtraction of the contribution of the all-*trans* form (Figure 2). The spectral comparison of 13C-ASR and AT-ASR upon the retinal isomerization at 77 K led to detection of the structural changes specific for each isomer. In addition, we revealed the hydrogen-bonding strengths of the Schiff base in each state using [ζ-^{15}N]lysine-labeled ASR.

Unphotolyzed State of 13C-ASR. We identified the N−D stretching vibration of the Schiff base at 2165 cm^{-1} for 13C-ASR (Figure 6a). We also identified the N−D stretching vibration of the Schiff base at 2163 and 2125 cm^{-1} for AT-ASR. The similar frequencies in 13C-ASR and AT-ASR indicate that the hydrogen-bonding strength of the Schiff base is nearly identical, being slightly stronger in AT-ASR. In the case of BR, the N−D stretching vibrations of the Schiff base were determined to be at 2171 and 2124 cm^{-1} (*29*). X-ray crystallographic structures of ASR and BR reported the presence of a water molecule in contact with the Schiff base (*14*, *33*). Therefore, similar hydrogen-bonding strength for 13C-ASR, AT-ASR, and BR suggests that the water molecule is a good hydrogen-bonding acceptor for the protonated Schiff base.

Interestingly, two peaks were observed for the N−D stretch of the Schiff base of AT-ASR (Figure 6c) and BR (*15*), while only one peak was observed for that of 13C-ASR (Figure 6a). Origins of the two peaks in BR, *p*pR, and AT-ASR have not been well understood. Multiple vibrational modes or structural heterogeneity is a possible source of the two N−D stretches. A single peak of the 13-*cis* form in ASR may be useful for understanding of the nature of this mode. The study of the 13-*cis*,15-*syn* form of BR is also in progress.

We previously found that water vibrations are entirely different between AT-ASR and BR, though both possess a water molecule between the Schiff base and its counterion (Asp75 for ASR or Asp85 for BR) (*14*, *33*). In the case of BR, we observed water O−D stretches at 2700−2150 cm^{-1} (*34*−*36*), whereas AT-ASR possesses water O−D stretches only at 2700−2600 cm^{-1} (Figure 7b) (*15*). We interpreted the absence of bands of strongly bound water molecules by the difference in geometry of the hydrogen bond. Namely, the $N-O_{water}-O_{counterion}$ (the Schiff base nitrogen, water oxygen, and oxygen of the counterion) angle is 83° and 106° in ASR and BR, respectively. As the consequence, if the water oxygen fully accepts a hydrogen bond of the Schiff base, the O−H group of water points toward the oxygen of Asp85 in BR, but not toward that of Asp75 in ASR. Such a small difference in the angle can possibly determine the hydrogen-bonding strength of water molecules. We did not observe strongly hydrogen-bonded water molecules for 13C-ASR in this study (Figure 7a). This is consistent with the above argument, because the X-ray crystal structure of ASR provides a similar position of the Schiff base, the water, and Asp75 for both isomers at 2.0 Å resolution (*14*).

We observed water O−D stretches of 13C-ASR at 2660 and 2553 cm^{-1} (Figure 7a), which correspond to O−H stretches at 3592 and 3481 cm^{-1}, respectively, from the spectral analysis of the O−H stretching vibrations in H_2O (not shown). The O−H stretches of AT-ASR corresponding to the O−D stretches at 2690, 2640, and 2608 cm^{-1} in Figure 7b are found at 3636, 3558, and 3530 cm^{-1}, respectively. Since only the water bridging the Schiff base and Asp75 is located close to the chromophore, it is a reasonable postulation that two water bands of ASR originate from O−D (O−H) stretches of this water molecule. In general, a water molecule has two O−H groups, and their frequencies are distributed in the wide 3700−2700 cm^{-1} region depending on their coupling and hydrogen-bonding strength (*37*). Gaseous water exhibits asymmetric and symmetric stretching modes at 3755 and 3657 cm^{-1}, respectively, and the stretching frequency is lowered as its hydrogen bonding becomes stronger (*38*). It must be noted that the hydrogen-bonding strengths of the two O−H groups are probably not equivalent in the restricted protein environment, which breaks the C_{2v}-type symmetry. In such C_S-type symmetry, one O−H is hydrogen bonded and the other O−H is unbonded, and their frequencies are widely split. That is the case for the bridged water of BR, where such decoupling of the two stretching modes occurs (*36*). Consequently, one O−D stretch of water is at 2171 cm^{-1}, while another O−D stretch of water is at 2636 cm^{-1}. We suggested that the former points toward Asp85, while the latter points toward Asp212 (*36*). Nonsymmetrical bonding of the water molecule in BR is presumably important for the function (*39*, *40*).

In the case of 13C-ASR, the frequency difference between the O−D stretches is about 100 cm^{-1}. Corresponding O−H stretches are also about 100 cm^{-1} different, being comparable to the gaseous water. Therefore, stretching vibrations of the water molecule are presumably coupled in 13C-ASR, where *anti*-symmetric and symmetric O−D stretches are located at 2660 and 2553 cm^{-1}, respectively. The situation is probably similar for AT-ASR, where two out of the three bands at 2690, 2640, and 2608 cm^{-1} originate from the O−D stretches of the bridging water. The presence of the additional water band indicates involvement of a more distant water upon formation of $AT-ASR_K$.

Photoisomerization Process of 13C-ASR in Comparison with That of AT-ASR. Upon light absorption in 13C-ASR, photoisomerization probably takes place at the C13═C14 (double) bond, leading from the 13-*cis*,15-*syn* to the all-*trans*,15-*syn* form. It is generally accepted that the primary K intermediate is a high-energy state for retinal proteins. Chromophore distortion is one of the characteristic features of such high energy state, and HOOP vibrations monitor the chromophore distortion. The appearance of numerous HOOP modes in $13C-ASR_K$ vs just two in $AT-ASR_K$ (Figure 3) implies that the chromophore distortion in $13C-ASR_K$ is distributed more widely along the polyene chain. In other words, chromophore distortion is more localized in the Schiff base region for $AT-ASR_K$. Such difference in HOOP modes

is presumably correlated with the other observations including amide I, cysteine S−H stretch, the Schiff base N−D stretch, and water O−D stretch modes, as discussed below.

Amide I vibrations of the α-helix were clearly observed for the transition from 13C-ASR to 13C-ASR_K as shown by the negative bands at 1662, 1655, and 1649 cm^{-1} in Figure 4a. This is reasonable because the retinal chromophore is surrounded by α-helices. In addition, the bands at 1634 (−)/1628 (+) cm^{-1} are also ascribable to amide I vibration. In contrast, fewer structural changes reported by amide I vibrations were observed for the transition from AT-ASR to AT-ASR_K as we reported previously (*15*). Instead, it was suggested that imide I vibration, possibly due to Pro206, was greatly altered (*15*). Several amide I changes observed only for 13C-ASR are consistent with the picture obtained from the HOOP analysis, suggesting that extensive structural changes take place in 13C-ASR_K.

No structural perturbation was observed for S−H groups of cysteines in 13C-ASR, whereas there is a negative band at 2547 cm^{-1} and a positive band at 2538 cm^{-1} for AT-ASR (Figure 5). This indicates that only the all-*trans* to 13-*cis* isomerization leads to the alteration of the local structure of a cysteine in ASR. We previously suggested that among the three cysteines of ASR, Cys203 in helix G is the most likely candidate for this band. Cys203 is near Pro206 and close to the Schiff base region. Replacement of Cys203 by Ala results in a red-shifted λ_{max} (553 nm) relative to the wild-type ASR (unpublished data). This suggests that the Schiff base region is more perturbed in AT-ASR_K than in 13C-ASR_K.

The N−D stretching frequency of the Schiff base in 13C-ASR_K (2351 cm^{-1}) is lower than that in AT-ASR_K (2483 cm^{-1}), though they are similar between 13C-ASR and AT-ASR. We thus assume that the hydrogen bond of the Schiff base is broken in AT-ASR_K but not in 13C-ASR_K. Consequently, the hydrogen-bonding network is destabilized in AT-ASR_K, and protein structural changes proceed through the network, where the L, M (deprotonation of the Schiff base), and O states can be produced from AT-ASR. In contrast, structural perturbation of the Schiff base region is smaller in 13C-ASR_K, where the structural changes are distributed more widely.

The number of observed water bands was two for 13C-ASR and three for AT-ASR (Figure 7). As discussed above, the two water bands in 13C-ASR are assignable to the water molecule in the Schiff base region. The presence of an additional water band indicates involvement of a more distant water upon formation of AT-ASR_K. The second nearest water molecule in the X-ray structure is located 8.3 Å from the Schiff base nitrogen in the structure of AT-ASR and 8.0 Å in the structure of 13C-ASR (*14*). That water is located between Trp176 and Phe213 in the cytoplasmic region. The third nearest water molecule in the X-ray structure is located 9.2 Å from the Schiff base nitrogen in the structure of AT-ASR and 9.7 Å in the structure of 13C-ASR (*14*). That water is located near Arg72 in the extracellular region. No water molecules are present near the polyene chain. Thus, water signals may also be consistent with the above view that the chromophore of 13C-ASR_K is distorted more widely along the polyene chain than that of AT-ASR_K, which has larger changes in the Schiff base region.

In conclusion, ASR accommodates both all-*trans*- and 13-*cis*,15-*syn*-retinal in the ground state according to the X-ray crystal structure (*14*). On the other hand, the present FTIR study revealed that protein structural changes upon retinal photoisomerization were significantly different between 13C-ASR and AT-ASR. They must trigger global protein structural changes in each photoreaction cycle, resulting in the photochromic behavior. The photochromic signaling mechanism of ASR has not been found, but we should be able to reveal such mechanism if the AT-ASR and 13C-ASR states differ in the binding affinity of the 14 kDa transducer. The other possibility is that the M state from the photocycle of AT-ASR, which is conformationally changed, would be the signaling state similar to other sensory rhodopsins.

REFERENCES

1. Lanyi, J. K. (1998) Understanding structure and function in the light-driven proton pump bacteriorhodopsin, *J. Struct. Biol. 124*, 164−178.
2. Essen, L. O. (2002) Halorhodopsin: light-driven ion pumping made simple?, *Curr. Opsin Struct. Biol. 12*, 516−522.
3. Sasaki, J., and Spudich, J. L. (2000) Proton transport by sensory rhodopsins and its modulation by transducer-binding, *Biochim. Biophys. Acta 1460*, 230−239.
4. Kamo, N., Shimono, K., Iwamoto, M., and Sudo, Y. (2001) Photochemistry and photoinduced proton-transfer by *pharaonis* phoborhodopsin, *Biochemistry (Moscow) 66*, 1277−1282.
5. Bieszke, J. A., Braun, E. L., Bean, L. E., Kang, S., Natvig, D. O., and Borkovich, K. A. (1999) The nop-1 gene of *Neurospora crassa* encodes a seven transmembrane helix retinal-binding protein homologous to archaeal rhodopsins, *Proc. Natl. Acad. Sci. U.S.A. 96*, 8034−8039.
6. Sineshchekov, O. A., Jung, K. H., and Spudich, J. L. (2002) Two rhodopsins mediate phototaxis to low- and high-intensity light in *Chlamydomonas reinhardtii*, *Proc. Natl. Acad. Sci. U.S.A. 99*, 8689−8694.
7. Nagel, G., Ollig, D., Fuhrmann, M., Kateriya, S., Musti, A. M., Bamberg, E., and Hegemann, P. (2002) Channelrhodopsin-1: a light-gated proton channel in green algae, *Science 296*, 2395−2398.
8. Okamoto, O. K., and Hastings, J. W. (2003) Novel dinoflagellate clock-related genes identified through microarray analysis, *J. Phycol. 39*, 519−526.
9. Jung, K. H., and Spudich, J. L. (2004) Microbial rhodopsins: Transport and sensory proteins throughout the three domains of life, in *CRC Handbook of Organic Photochemistry and Photobiology* (Horspool, W. M., and Lenci, F., Eds.) 2nd ed., Sect. II, pp 124/1−124/11, CRC Press, Boca Raton, FL.
10. de la Torre, J. R., Christianson, L. M., Beja, O., Suzuki, M. T., Karl, D. M., Heidelberg, J., and DeLong, E. F. (2003) Proteorhodopsin genes are distributed among divergent marine bacterial taxa, *Proc. Natl. Acad. Sci. U.S.A. 100*, 12830−12835.
11. Beja, O., Aravind, L., Koonin, E. V., Suzuki, M. T., Hadd, A., Nguyen, L. P., Jovanovich, S. B., Gates, C. M., Feldman, R. A., Spudich, J. L., Spudich, E. N., and DeLong, E. F. (2000) Bacterial rhodopsin: evidence for a new type of phototrophy in the sea, *Science 289*, 1902−1906.
12. Giovannoni, S. J., Bibbs, L., Cho, J. C., Stapels, M. D., Desiderio, R., Vergin, K. L., Rappe, M. S., Laney, S., Wilhelm, L. J., Tripp, H. J., Mathur, E. J., and Barofsky, D. F. (2005) Proteorhodopsin in the ubiquitous marine bacterium SAR11, *Nature 438*, 82−85.
13. Jung, K. H., Trivedi, V. D., and Spudich, J. L. (2003) Demonstration of a sensory rhodopsin in eubacteria, *Mol. Microbiol. 47*, 1513−1522.
14. Vogeley, L., Sineshchekov, O. A., Trivedi, V. D., Sasaki, J., Spudich, J. L., and Luecke, H. (2004) *Anabaena* sensory rhodopsin: a photochromic color sensor at 2.0 Å, *Science 306*, 1390−1393.
15. Furutani, Y., Kawanabe, A., Jung, K. H., and Kandori, H. (2005) FTIR spectroscopy of the all-*trans* form of *Anabaena* sensory rhodopsin at 77 K: hydrogen bond of a water between the Schiff base and Asp75, *Biochemistry 44*, 12287−12296.

16. Sineshchekov O. A., and Spudich J. L. (2004) Light-induced intramolecular charge movements in microbial rhodopsins in intact *E. coli* cells, *Photochem. Photobiol. Sci. 3*, 548−554.
17. Furutani, Y., Shibata, M., and Kandori, H. (2005) Strong hydrogen-bonded water molecules in the Schiff base region of rhodopsins, *Photochem. Photobiol. Sci. 4*, 661−666.
18. Kandori, H., Shimono, K., Sudo, Y., Iwamoto, M., Shichida, Y., and Kamo, N. (2001) Structural changes of *pharaonis* phoborhodopsin upon photoisomerization of the retinal chromophore: infrared spectral comparison with bacteriorhodopsin, *Biochemistry 40*, 9238−9246.
19. Shimono, K., Furutani, Y., Kamo, N., and Kandori, H. (2003) Vibrational modes of the schiff base in *pharaonis* phoborhodopsin, *Biochemistry 42*, 7801−7806.
20. Shimono, K., Ikeura, Y., Sudo, Y., Iwamoto, M., and Kamo, N. (2001) Environment around the chromophore in *pharaonis* phoborhodopsin: mutation analysis of the retinal binding site, *Biochim. Biophys. Acta 1515*, 92−100.
21. Imamoto, Y., Shichida, Y., Hirayama, J., Tomioka, H., Kamo, N., and Yoshizawa, T. (1992) Chromopore configuration of *pharaonis* phoborhodopsin and its isomerization on photon absorption, *Biochemistry 31*, 2523−2528.
22. Shineshchekov, O. A., Trivedi, V. D., Sasaki, J., and Spudich, J. L. (2005) Photochromicity of *Anabaena* sensory rhodopsin, an atypical microbial receptor with a *cis*-retinal light-adapted form, *J. Biol. Chem. 280*, 14663−14668.
23. Pettei, J. M., Yudd, P. A., Nakanishi, K., Henselman, R., and Stoeckenius, W. (1977) Identification of retinal isomers isolated from bacteriorhodopsin, *Biochemistry 16*, 1955−1959.
24. Aton, B., Doukas, A. G., Callender, R. H., Becher, B., and Ebrey, T. G. (1977) Resonance Raman studies of the purple membrane, *Biochemistry 16*, 2995−2999.
25. Roepe, P. D., Ahl, P. L., Herzfeld, J., Lugtenburg, J., and Rothchild, K. J. (1988) Tyrosine protonation changes in bacteriorhodopsin: A Fourier transform infrared study of BR548 and its primary photoproduct, *J. Biol. Chem. 263*, 5110−5117.
26. Mathies, R. A., Smith, S. O., and Pollard, W. T. (1987) in *Biological applications of Raman spectroscopy: Resonance Raman spectra of polyenes and aromatics* (Spiro, T. G., Ed.) pp 59−108, John Wiley and Sons, New York.
27. Rodman-Gilson, H. S., Honig, B., Croteau, A., Zarrilli, G., and Nakanishi, K. (1988) Analysis of the factors that influence the C═N stretching frequency of polyene Schiff bases. Implications for bacteriorhodopsin and rhodopsin, *Biophys. J. 53*, 261−269.
28. Baasov, T., Friedman, N., and Sheves, M. (1987) Factors affecting the C═N stretching in protonated retinal Schiff base: a model study for bacteriorhodopsin and visual pigments, *Biochemistry 26*, 3210−3217.
29. Kandori, H., Belenky, M., and Herzfeld, J. (2002) Vibrational frequency and dipolar orientation of the protonated Schiff base in bacteriorhodopsin before and after photoisomerization, *Biochemistry 41*, 6026−6031.
30. Mogi, T., Stern, L. J., Marti, T., Chao, B. H., and Khorana, H. G. (1988) Aspartic acid substitutions affect proton translocation by bacteriorhodopsin, *Proc. Natl. Acad. Sci. U.S.A. 85*, 4148−4152.
31. Kandori, H., Shimono, K., Shichida, Y., and Kamo, N. (2002) Interaction of Asn105 with the retinal chromophore during photoisomerization of *pharaonis* phoborhodopsin, *Biochemistry 41*, 4554−4559.
32. Kandori, H., Kinoshita, N., Yamazaki, Y., Maeda, A., Shichida, Y., Needlman, R., Lanyi, J. K., Bizounok, M., Herzfeld, J., and Lugtenburg, J. (1999) Structural change of threonine 89 upon photoisomerization in bacteriorhodopsin as revealed by polarized FTIR spectroscopy, *Biochemistry 38*, 9676−9683.
33. Luecke, H., Schobert, B., Richter, H. T., Cartailler, J. P., and Lanyi, J. K. (1999) Structure of bacteriorhodopsin at 1.55 Å resolution, *J. Mol. Biol. 291*, 899−911.
34. Kandori, H., and Shichida, Y. (2000) Direct observation of the bridged water stretching vibrations inside a protein, *J. Am. Chem. Soc. 122*, 11745−11746.
35. Shibata, M., Tanimoto, T., and Kandori, H. (2003) Water molecules in the Schiff base region of bacteriorhodopsin, *J. Am. Chem. Soc. 125*, 13312−13313.
36. Shibata, M., and Kandori, H. (2005) FTIR studies of internal water molecules in the Schiff base region of bacteriorhodopsin, *Biochemistry 44*, 7406−7413.
37. Eisenberg, D., and Kauzmann, W. (1969) *The structure and properties of water*, Oxford University Press, London.
38. Kandori, H. (2000) Role of internal water molecules in bacteriorhodopsin, *Biochim. Biophys. Acta 1460*, 177−191.
39. Tanimoto, T., Furutani, Y., and Kandori, H. (2003) Structure changes of waer in the Schiff base region of bacteriorhodopsin: proposal of a hydration switch model, *Biochemstry 42*, 2300−2306.
40. Kandori, H. (2004) Hydration switch model for the proton transfer in the Schiff base region of bacteriorhodopsin, *Biochim. Biophys. Acta 1658*, 72−79.

BI052324B